The concentration, source and deposition flux of inorganic nitrogen in atmospheric particles at a coastal site in northern China during dust events

Jianhua Qi[1], Xiaohuan Liu[1], Xiaohong Yao[1], Ruifeng Zhang[1], Xiaojing Chen[1], Xuehui Lin[2],Huiwang Gao[1],Ruhai Liu[1]

[1]Key Laboratory of Marine Environment and Ecology, Ministry of Education, Ocean University of China, Qingdao, 266100, China

[2]Qingdao Institute of Marine Geology, Qingdao, 266100, China

Correspondence to: Jianhua Qi (qjianhua@ouc.edu.cn)

Abstract. Asian dust has been reported to carry anthropogenic reactive nitrogen during the transport from source areas to the oceans. In this study, we attempted to characterize the NH_4^+ and NO_3^- in atmospheric particles collected at a coastal site in northern China during spring dust events from 2008 to 2011. Based on the mass concentrations of NH_4^+ and NO_3^- in each total suspended particle (TSP) sample, the samples can be classified into two groups: in Category 1, the concentrations of NH_4^+ and NO_3^- were 20%-440% higher in dust day samples relative to samples collected immediately before or after dust event, while in Categories 2 and 3, these concentrations decreased by10-75% in the dust day samples. For these two groups, NH_4^+in dust day samples waspresent in the form of ammonium salts externally co-existing with dust aerosols or the residual of incomplete reactions between ammonium salt and carbonate salts. The NO_3^- in the dust day samples was attributed to interactions between anthropogenic air pollutants and dust particles during dust transport from the source zone to the reception site. Back trajectory analysis showed that the concentrations of NH_4^+ and NO_3^- were apparently affected by the transport distance prior to the reception site, the mixing layer depth and the residence time across highly polluted regions during transport. The positive matrix factorization (PMF) receptor model results showed that the contribution of soil dust increased from 23% to 36% (90% of the residuals<3.0 and r^2=0.97) on dust days with decreasing contributions of local anthropogenic inputs, especially secondary aerosols. The dry deposition flux of atmospheric particulates increased from 2,800±700 mg/m^2/month on non-dust comparison days to 16,800±15,900 mg/m^2/month on dust days. The dry deposition flux of particulate inorganic nitrogen increased by 9-285% in Category 1. The average

dry deposition flux of nitrate decreased by 46%-73% in Category 2, while that of ammonium decreased by 47% in Category 3. The estimated dust deposition flux varied greatly from event to event. Overall, a slight increase in dry deposition flux of particulate inorganic nitrogen associated with dust events in this study relative to values in the literature may reflect the combined effect of anthropogenic nitrogen emissions and the occurrence of natural dust events.
Keywords: aerosols, nitrogen, dust, source apportionment, dry deposition flux

1 Introduction

Reactive nitrogen carried in dust particles can be transported over long distances, and the nitrogen deposition in oceans has been recognized as an important external source of nitrogen supporting phytoplankton growth (Duce et al., 2008; Zhang et al., 2010b). This hypothesis has been evaluated in incubation experiments, in situ experiments, and through the use of satellite observational data (Shi et al., 2012; Guo et al., 2012; Liu et al., 2013; Tan and Wang, 2014). For example, Tan and Wang (2014) found that a phytoplankton bloom with a nearly four-fold increase in chlorophyll concentrations occurred 10-13 days after dust deposition. In addition, Banerjee and Kumar (2014) hypothesized that dust-induced episodic phytoplankton blooms are important to the interannual variability of chlorophyll in the Arabian Sea. Dramatic changes have occurred in the reactive nitrogen in anthropogenic emission in the last three decades, e.g., large increases in NH_3 and NO_x in emissions in China and other developing countries in Asia and a substantial decrease in emissions in Europe (Grice et al., 2009; Liu et al., 2017; Ohara et al., 2007; Skjøth and Hertel, 2013). These changes may greatly affect the nitrogencarried by dust particles, but few recent studies have examined this issue.

Asian dust is one of the main components of dust worldwide. Asian dust has been reported to cross over the mainland and the marginal seas of China and reach as far as the remote northern Pacific Ocean (Zhang and Gao, 2007; Tan and Wang, 2014). During the long-range transport, dust particles may mix with anthropogenic gas and particles, consequently resulting in complicated chemical reactions (Cui et al., 2009; Wang et al., 2011; Wang et al., 2016, Wang et al., 2017). However, the extent of these chemical reactions varies widely and depends on the meteorological conditions, such as cloud fraction, wind speed, relative humidityand atmospheric circulation (Yang et al., 2002; Li et al., 2014; Ma et al., 2012). For example, a few studies have shown that the concentrations of atmospheric particulate NO_3^- and NH_4^+ on dust storm days were 2-5 times larger than those prior to the events in Beijing (Liu et al.,

2014; Liu and Bei, 2016). Xu et al. (2014) also reported that concentrations of particulate SO_4^{2-} and NO_3^- simultaneously increased during dust storm events along the northern boundary of the Tibetan Plateau. Fitzgerald et al. (2015) found that almost all Asian dust observed in Korea contained considerable amounts of nitrate and proposed that the dust from the Gobi and Taklamakan Deserts probably mixed and reacted with anthropogenic air pollutants during transport over the Asian continent. Although increased concentrations of NO_3^- and NH_4^+ in aerosol particles were observed on dust storm days in northern China relative to those non-dust days prior to the dust storm events, Zhang et al. (2010a) also found that the concentrations of the two species were associated with the intensity of the dust storm, i.e., the stronger dust storms corresponded to the smaller increases. In other words, lower NO_3^- and NH_4^+ concentrations occurred during strong dust storm events than during weak dust events (Zhang et al., 2010a).

On the other hand, some studies reported the reverse result. For example, at Yulin, a rural site near the Asian dust source region, the concentration of NO_3^- in atmospheric aerosols on dust days was significantly lower in comparison to the concentration measured immediately before or after the event, as a result of the dilution effect (Wang et al., 2016). Even in Shanghai, a mega city located at a few thousands kilometers from dust source zones in China, the concentrations of NO_3^- and NH_4^+ were notably lower in the observed dust plumes than in a polluted air parcel observed immediately prior to the dust events (Wang et al., 2013). Li et al. (2014) also found that the concentrations of nitrate and ammonium decreased on dust storm days with a decreasing ratio of the total soluble inorganic ions to $PM_{2.5}$ in the Yellow River Delta, China. When dust was rapidly transported from desert regions without passing through major urban areas and lingering over the Yellow Sea, the concentrations and size distributions of nitrate and ammonium had no significant variation in heavy Asian dust (AD) plumes (Kang et al., 2013).

The contradictory results highlight the importance of investigating the concentrations of ammonium and nitrate in atmospheric particles during dust events based on a larger database. In this study, we collected atmospheric aerosol particles during and prior to (or after,when no sample was collected prior to) dust events at a coastal site adjacent to the Yellow Sea during the spring from 2008 to 2011 when smaller outbreak peaks of dust storms occurred. We measured the concentrations of inorganic nitrogen in the samples as well as other components to facilitate our analysis. We first characterized the concentrations of inorganic nitrogen concentrations in various dust events relative to the concentrations

in samples collected either prior to or after the events. We then conducted source apportionment to quantify their sources. Finally, we calculated the deposition flux of atmospheric particulate inorganic nitrogen during dust events and compared the results with the values in the literature in order to update the flux values due to dynamic changes in anthropogenic emissions and other factors.

2 Experimental methods

2.1 Sampling

Fig. 1 shows the sampling site, which is situated at the top of a coastal hill (Baguanshan) in Qingdao in northern China (36° 6' N, 120° 19' E, 77 m above sea level) and is approximately 1.0 km from the Yellow Sea to the east. A high-volume air sampler (Model KC-1000, Qingdao Laoshan Electronic Instrument Complex Co., Ltd.) was set up on the roof of an two-story office buildingto collect total suspended particle (TSP) samples on quartz microfiber filters (Whatman QM-A) at a flow rate of 1 m^3/min. Prior to the sampling, the filters were heated at 450°C for 4.5 h to remove organic compounds. Our sample collection strategy involved collecting dust samples representing long-range transported particles. We followed the definition of dust events adopted in the regulations of surface meteorological observations of China (CMA, 2004; Wang et al., 2008) and identified dust events based on the meteorological records (Weather Phenomenon) of Qingdao from Meteorological Information Comprehensive Analysis and Process System (MICAPS) of the China Meteorological Administration. Each dust sample was collected over 4 hrs, and the sampling started only when the PM_{10} and dust mass concentration available on the website (http://www-cfors.nies.go.jp/~cfors/;http://www.qepb.gov.cn/m2/) had increased greatly. This approach made the dust sample more representative relative to urban background. For dust events with durations of less than one day, only one sample was collected. For dust events with durations greater than one day, a 4-hr dust sample was collected once per day. Table 1 lists the sampling information. Based on the forecast, we also collected aerosol particle samples immediately before or after the dust event for comparison. These comparison samples were further classified into sunny day samples, cloudy day samples and post-dust samples. The post-dust samples were collected under clear and sunny weather conditions and low PM_{10} mass concentrations.

Since Asian dust events at the sampling site mostly occur in the spring, we collected samples during

every spring, i.e., from March to May, from 2008-2011. A smaller peak in Asian dust was observed in eastern China in 2008-2011, which followed a larger peak in 2000-2003 during this century (Fig. 6). Overall, a total of 14 sets of dust samples and 8 sets of comparison samples were collected for this study.

To facilitate the coastal sampling data analysis, sand samples were collected at the Zhurihe site (42°22'N, 112°58'E) in the Hunshandake Desert, one of main Chinese sanddeserts, in April 2012. Sand samples were packed in clean plastic sample bags and were stored below -20°C before the transfer. An ice-box was used to store the samples during transport to the lab for chemical analysis.

2.2 Analysis

The aerosol samples were allowed to achieve equilibrium in a air-conditioned chamber at a constant relative humidity and temperaturefor 24hrs before weighing. The sample membranes were then cut into several portions for analysis. One portion of each aerosol sample was ultrasonically extracted with ultra-pure water in an ice water bath, and the concentration of inorganic water-soluble ions was determined using ICS-3000 ion chromatography (Qi et al., 2011). The sand samples collected at the Zhurihe site were analyzed using the same procedure. We refer to dissolved inorganic nitrogen (DIN), the sum of nitrate and ammonium, in the later discussion due to the very low concentration of nitrite in the samples.

One portion of each aerosol filter was cut into 60 cm^2 pieces and digested with HNO_3+$HClO_4$+HF (5:2:2 by volume) at 160°C using an electric heating plate. A blank membrane was also analyzed using the same procedure to ensure analytical precision. The concentrations of Cu, Zn, Cr, Sc and Pb were measured using inductively coupled plasma mass spectrometry (Thermo X Series 2), while the concentrations of Al, Ca, Fe, Na and Mg were measuredusing inductively coupled plasmaatomic emission spectroscopy (IRIS Intrepid II XSP). The membrane blanks have been corrected for in the calculation of the metal concentrations.

One portion of each aerosol sample was digested with an HNO_3 solution (10% HNO_3, 1.6 M) at 160°C for 20 min in a microwave digestion system (CEM, U.S.). The Hg and As in sample extracts were analyzed following the U.S. Environmental Protection Agency method 1631E (U.S. EPA, 2002) using cold vapor atomic fluorescence spectrometry (CVAFS). The detection limits, precisions and recoveries of water-soluble ions and metal elements are listed in Table 2.

147 **2.3 Computational modeling**

148 The enrichment factor of metal elementswas given by

$$EFi = \frac{\left(X_i / X_{\mathrm{Re}}\right)_{aerosols}}{\left(X_i / X_{\mathrm{Re}}\right)_{crust}} \quad (1)$$

149

150 where subscripts *i* and *Re* refer to the studied metal and the reference metal; $(X_i/X_{Re})_{aerosols}$ is the
151 concentration ratio of metal *i* to metal *Re* in the aerosol samples; and $(X_i/X_{Re})_{crust}$ is the ratio of metal *i*
152 to metal *Re* in the Earth crust. For the calculation of the enrichment factor of the metal elements,
153 scandium was used as the reference element (Han et al., 2012), and the abundance of elements in the
154 Earth's crust given by Taylor (1964) was adopted.

155 The 72-h air mass back trajectories were calculated for each TSP sample using TrajStat software
156 (Wang et al., 2009) and the NOAA GDAS archive data (http:// www.arl.noaa.gov/ready/hysplit4.html).
157 The air mass back trajectories were calculated at an altitude of 1500 m to identify the dust origin.

158 The positive matrix factorization (PMF) is a commonly used receptor modeling method. This model
159 can quantify the contribution of sources to samples based on the composition or fingerprints of the
160 sources (Paatero and Tapper, 1993; Paatero, 1997). The measured composition data can be represented
161 by a matrix X of *i* by *j* dimensions, in which *i* number of samples and *j* chemical species were
162 measured, with uncertainty *u*. X can be factorized as a source profile matrix (F) with the number of
163 source factors (*p*) and a contribution matrix (G) of each source factor to each individual sample, as
164 shown in Equation 2.

$$X_{ij} = \sum_{k=1}^{p} G_{ik} F_{kj} + E_{ij} \quad (2)$$

165

166 where *Eij* is the residual for species *j* of the i-th sample.

167 The aim of the model is to minimize a objective function Q, which was calculated from the residual
168 and uncertainty of all samples (Equation 3), to obtain the most optimal factor contributions and
169 profiles.

$$Q = \sum_{i=1}^{n} \sum_{j=1}^{m} (E_{ij}/u_{ij})^2 (3)$$

170

171 The EPA PMF 3.0 model was used to obtain the source apportionment of atmospheric particulates on
172 dust and comparison days. The correlation coefficient between the predicted and observed
173 concentrations was 0.97.

174 Dry deposition velocities were obtained using Williams' model (Williams, 1982) by accounting for

175 particle growth (Qi et al., 2005). Williams' model is a two-layer model used to calculate the dry
176 velocity of size-segregated particles over the water. In an upper layer below a reference height (10 m),
177 the deposition of aerosols particles is governed by turbulent transfer and gravitational settling. In the
178 deposition layer, gravitational settling of particles is affected by particle growth due to high relative
179 humidity. To obtain the deposition velocity of different particle size, Williams' model needs many input
180 parameters, such as the wind speed at 10 m height (U_{10}), air/water temperature, and relative humidity.
181 Relative humidity, air temperature and U_{10} obtained from the National Centers for Environmental
182 Prediction (NCEP) were used in this study. Surface seawater temperature data was collected from the
183 European Centre for Medium-Range Weather Forecasts (ECMWF). The meteorological and seawater
184 temperature data had a six-hour resolution. According to a previously reported method (Qi et al., 2013),
185 the dry deposition fluxes of the particles and the nitrogen species were calculated for dust and
186 comparison days.

187 The CMAQ model (v5.0.2) was applied over the East Asia area to simulate the concentrations of
188 PM10, NO_x and NH_3 for 14 samples collected during 11 dust events. The simulated domain contains
189 164×97 grid cells with a 36 km spatial resolution. The vertical resolution includes 14 layers from
190 surface to tropopause, with the first model layer height of 36m above the ground level. The
191 meteorological fields were generated by the Weather Research and Forecasting (WRF) Model (v3.7).
192 Considering that the simulated area is connected to the Yellow Sea, the CB05Cl chemical mechanism
193 was chosen to simulate the gas-phase chemistry. The emissions of NO_X and NH_3 over East Asia for
194 each dust event were also modeled using the CMAQ model according to the emission inventory in
195 2008, which was generated by extrapolating the 2006 activity data to the year 2008 using the method
196 described by Zhang et al.(2009). Initial conditions (ICONs) and boundary conditions were generated
197 from a global chemistry model of GEOS-CHEM. All the dust events simulations are performed
198 separately, each with a 1-week spin-up period to minimize the influence of the ICONs. Validation of
199 the application of the CMAQ model in China has been reported by Liu et al. (2010a, b). The spatial
200 distribution of PM10 concentrations for each dust event was consistent with the model results of dust
201 by the Chemical Weather Forecast System (CFORS) by Uno et al. (2003).

202 **2.4 Other data sources and statistical analysis**

203 Meteorological data were obtained from the Qingdao Meteorological Administration

(http://qdqx.qingdao.gov.cn/zdz/ystj.aspx) and the MICAPS of the Meteorological Administration of China. Different weather characteristics, such as sunny days, cloudy days and dust days, were defined according to information from the MICAPS and Qingdao Meteorological Administration. According to the altitude, longitude and latitude of the 72 h air mass back trajectory of each dust sample, the pressure level, temperature and relative humidity data along the path of the air mass were derived from the NCEP/NCAR re-analysis system (http://www.esrl.noaa.gov/psd/data/gridded/data.ncep.reanalysis.html) for each sample. The mixed layer depth during the air mass transport of dust samples was obtained from the HYSPLIT Trajectory Model (http://ready.arl.noaa.gov/hypub-bin/trajasrc.pl) using the same method. Spearman correlation analysis was applied to examine the relationships of nitrate and ammonium with transport parameters, and P values of <0.05 were considered to be statistically significant.

3 Results and discussion

3.1 Characterization of aerosol samples collected during dust events

To support our analysis, the dust intensity and influence range of the dust events modeled by Uno et al. (2003) were analyzed, and the spatial distributions of dust concentration over East Asia during each dust sampling day are shown in Fig. 2 and Fig. S3. Almost all dust events originated in northern or northwestern China and passed over the sampling site. However, Sample 20110415 was judged to be local blowing dust because no correspondinghigh dust concentrations were observed in the dust source areas; this sample was therefore excluded from further analysis.

Before characterizing the inorganic nitrogen in atmospheric particles from the Baguanshan site, we first examined the mass concentrations of TSP samples and the concentrations of crustal and anthropogenic metals to compare samples collected on dust days and immediately before or after days. The comparative results are highlighted below. For these comparison samples, the TSP mass concentrations ranged from 94 to 275 $\mu g \cdot m^{-3}$, with an average of 201 $\mu g \cdot m^{-3}$ (Fig. 2). The TSP mass concentration increased substantially to 501-3857 $\mu g \cdot m^{-3}$ in dust day samples, with an average of 1140.2 $\mu g \cdot m^{-3}$. In each dust day-comparison day sample pair, the mass concentration of TSPs increased by 80-1303%, with a median value of 537%. A similar increase was present in the crustal elements in each pair of samples. For example, the mean concentrations of Sc, Al, Fe, Ca and Mg increased by over

a factor of four in dust day samples relative to comparison samples. In addition, the enrichment factors (EF) of Al, Fe, Ca, and Mg were less than three in dust day samples but were less than 14 in comparison samples (Table 3). Lower values are indicative of elements from the primarily crustal origin. Although the average mass concentrations of anthropogenic elements, such as Cu, Pb, Zn, Cr, Hg and As, in dust day samples increased 107% to 722% relative to those in comparison samples, the EF of the anthropogenic metal elements decreased in the dust day samples. This pattern indicates a decreasing relative contribution of anthropogenic sources to the total TSP mass in dust day samples.

3.2 Concentrationsof inorganic nitrogen in dust day samples

When the mass concentrations of NH_4^+ and NO_3^- in each pair of TSP samples were compared, the concentrations of NH_4^+ increased by 45%-487% in some dust day samples (20080301, 20080315, 20090316, 20100315, 20100320, 20100315. 20110415 and 20110418), but decreased by 28-84% in other dust day samples (Fig.3, Table S1). The same was generally true for the measured concentrations of NO_3^-.

Considering the relative values of NH_4^+ and NO_3^- in dust day samples relative to comparison samples, the dust day samples can be classified into three categories (Table 4). In Category 1, the mass concentrations of NH_4^+ and NO_3^- were larger in dust day sample than in the comparison samples. In Category 2, the reverse was true. In Category 3, the mass concentrations of NO_3^- were lower in the dust samples than in the comparison samples, whereas the reverse was true for NH_4^+.

Considering that the Yellow Sea was mainly affected by dust storms from the Hunshandake Desert (Zhang and Gao, 2007), we compared our observations with the sand particles collected from this desert (Table 5). The relative mass concentrations of nitrate and ammonium to the total mass of sand particles were very low, i.e., less than 81μg/g, approximately three orders of magnitude less than the corresponding values in our dust samples. Moreover, the values obtained from atmospheric aerosols at Duolun (Cui, 2009) and Alxa Right Banner (Niu and Zhang, 2000) were also more than one order of magnitude lower than the corresponding values in this study (Table 5). This suggested that NO_3^- and NH_4^+ observed in the dust day samples were very likely due to interactions and mixing between anthropogenic air pollutants and dust particles during transport from the source zone to the reception site (Cui et al., 2009,Wang et al., 2011; Wu et al., 2016). However, along the different transport paths of

Asian dust, air pollutant emissions, meteorological conditions, chemical reactions, and other factors can affect the abundance of NH_4^+ and NO_3^- in atmospheric particles. These factors can vary greatly among different dust events, hence leading to the three different categories.

3.3 Theoretical analysis of the three categories

Ammonium salts are common in atmospheric particles with diameters of less than 2 μm (Yao et al., 2003; Yao and Zhang, 2012). Gas-aerosol thermodynamic equilibrium is widely assumed to be fully attained for inorganic ions, including ammonium salts in $PM_{2.5}$, in all regional air quality modeling studies. Reasonably good agreements between ammonium salt modeling results and observations reported in literature support the validity of this assumption (Chen et al., 2016; Penrodet al., 2014; Walker et al., 2012). Assuming that thermodynamic equilibrium had been attained by the ammonium salts in Category 1, the reactions between carbonate salts and ammonium salts, such as 1) $(NH_4)_2SO_4$+ $CaCO_3 \Rightarrow CaSO_4 + NH_3$ (gas) +CO_2 (gas) +H_2O and 2) $2NH_4NO_3$+ $CaCO_3 \Rightarrow Ca(NO_3)_2 + 2NH_3$ (gas) +CO_2 (gas) +H_2O, will release NH_3 (gas) until $CaCO_3$ has been completely used up. During dust events, much high concentrations of Ca^{2+} were observed, and high $CaCO_3$ concentrations were therefore expected. When Category 1 was considered alone and one exterior sample was excluded, a good correlation however, was obtained for $[NH_4^+]_{equivalent\ concentration}=0.98*[NO_3^-+SO_4^{2-}]_{equivalent\ concentration}$($R^2$=0.83, P<0.05). The good correlation together with the slope of 1 strongly indicated that the NO_3^- and SO_4^{2-} were almost completely associated with NH_4^+ in these dust day samples. The formation of $CaSO_4$ and/or $Ca(NO_3)_2$ was probably negligible. Thus, ammonium salt aerosols may externally co-exist with dust aerosols in these dust day samples. In the exterior sample collected on 21 March 2010, $[NH_4^+]$ only accounted for ~70% of the observed $[NO_3^-+SO_4^{2-}]$ in equivalent concentration. This result suggested that ~30% of ($NO_3^-+SO_4^{2-}$) may be associated with dust aerosols via the formation of metal salts of the two species. The hypothesis was supported by the correlation result, i.e., NO_3^- was positively correlated with NH_4^+ and Cu, and SO_4^{2-} was correlated with K^+, Na^+ and Mg^{2+} (Fig.S4). Note that only samples in Category 1 showed NH_4^+ to be negatively correlated with Ca^{2+} (Fig.S4).

For Category 2, no correlation between $[NH_4^+]_{equivalent\ concentration}$ and $[NO_3^-+SO_4^{2-}]_{equivalent\ concentration}$ existed. When Category 2 was considered alone and one exterior sample was excluded, the equivalent ratios of NH_4^+ to $NO_3^-+SO_4^{2-}$ were generally much smaller than 1, suggesting that a larger fraction of

289 NO_3^-+SO_4^{2-} may exist as metal salts due to reactions of their precursors with dust aerosols. NO_3^- and
290 SO_4^{2-} showed no correlations with NH_4^+ but did show significant correlations with Pb (Fig.S4),
291 implying that NO_3^-+SO_4^{2-} existed as metal salts. The average concentration of Ca^{2+} in Category 2
292 (0.43±0.40μg/m^3) was clearly higher than that in Category 1 (Ca^{2+}: 0.17±0.04μg/m^3), implying the
293 probable formation of $CaSO_4$ and/or $Ca(NO_3)_2$ and the release of NH_3 (gas), resulting in a decrease in
294 NH_4^+. However, the concentration of total Ca was 1.11±0.70 μg/m^3 in Category 1 and 0.74±0.49 μg/m^3
295 in Category 2. In Category 1, NO_3^- was negatively correlated with SO_4^{2-} (Fig.S4), suggesting
296 competition for NH_3 under NH_3-poor dust days during long-range transport. However, NO_3^- was
297 positively correlated with SO_4^{2-} in Category 2. The latter relationship can be explained by the fact that
298 the amount of $CaCO_3$ was sufficient to absorb the precursors of both SO_4^{2-} and NO_3^-. Due to the
299 absence of TSP concentration data along the transport pathway, we compared TSP concentrations at the
300 sampling site and found that the average value of Category 2 (1391±981 μg/m^3) was substantially
301 higher than that of Category 1 (591±158 μg/m^3). This implied that dust events in Category 2 were even
302 stronger. Note that the NO_2 concentrations in Category 2 (1.35±2.45 μg/m^3) were lower or comparable
303 to those in Category 1 (1.51±2.16 μg/m^3). The potential formation of nitrate metal salts was expected to
304 be similar between the two categories, while favorable formation conditions for ammonium nitrate
305 greatly increased the mass concentrations of nitrate and the contributions to the TSPs in Category 1.

306 Overall, the higher ammonium concentrations observed in the dust day samples in Category 1 were
307 likely associated with external co-existence of ammonium salt aerosols. However, the lower
308 concentrations in Category 2 were likely due to unfavorable conditions for forming ammonium salts.
309 The observed ammonium was just the residual of incomplete reactions between preexisting ammonium
310 salt and carbonate salts. More discussion on this issue will be presented in Section 3.4.

311 **3.4 Influence of transport pathways on particulate inorganic nitrogenin dust samples**

312 The calculated air mass trajectoriesof 13 out of 14 samplesshowed that the air mass originated from
313 Inner Mongolia, China (Fig. 5), generally consistent with the results by Zhang and Gao (2007). The
314 remaining one originated from Northeast China. Figs. 6 and 7 show a few areas with high emissions of
315 NO_x and NH_3, e.g., Liaoning, Beijing-Tianjin-Hebei, Shandong, Henan and Jiangsu in China. The
316 calculated trajectories showed that all the air mass passed over parts of these highly polluted regions

and experienced different residence time in these regions. In Fig. 5, except for the one exterior sample, all trajectories in Category 1 showed that the air masses were transported from either the north or northwest over the continent. In Category 2, the air masses crossed over the sea for 94-255 km prior to arriving at the reception site. NH_3-poor conditions in the marine atmosphere disfavored the formation and existence of ammonium nitrate. On the other hand, the humid marine conditions might have enhanced particle-particle coagulation and might have led to the release of NH_3 via reactions between preexisting ammonium salts and carbonate salts. Moreover, we also examined the links among the measured concentrations of particulate ammonium and nitrate, the mixing layer along the back trajectories, and the residence time of air masses crossing over the highly polluted zones. The results supported our hypothesis, i.e., ammonium salts mostly co-existed with dust aerosols externally. For example, except for 20080425, all dust day samples mostly traveled at an altitude above the mixing layer before mixing down to ground level. For most sampling days in Category 1, the average mixing layer was less than 900 m, favoring the trapping of locally emitted anthropogenic air pollutants in the mixing layer. In addition, the air masses at this elevation apparently moved slowly and took over 10 hr to cross over the highly polluted area. Even lower speeds were expected for air masses at the bottom of the mixing layer, as wind speed decreases with height. Except for exterior samples, the sampling days in Category 2 featured a mixing layer that was, on average, higher than 900 m. The air masses at this elevation took less than 10 hr to cross over the highly polluted areas and generally had higher speeds. Theoretically, a lower mixing layer and a lower wind speed favored the accumulation of air pollutants and the formation of ammonium nitrate to some extent. The transport of dust air masses above the mixing layer reduced the possibility for internal mixing of ammonium salts and reaction with dust aerosols along the long transport path. The shorter time for dust air masses mixing down to ground level before arriving at the reception site also increased the possibility for external co-existence between ammonium salt aerosols and dust aerosols in Category 1. The reverse could be argued to explain the observations for Category 2. The correlation analysis results in Table S2 indirectly support these conclusions. In fact, previous studies proposed that nitrate is rarely formed on the surface of dust particles (Zhang and Iwasaka, 1999). Therefore, much lower nitrate concentrations were observed in Category 2. Noted that the exteriors with ID of 20110415 and 20110502 have not yet been explained.

3.5 Source apportionment of aerosols duringdust and non-dust events

346 The sources of atmospheric aerosols on dust and comparison days were determined by the PMF
347 modeling (Paatero and Tapper, 1993; Paatero, 1997). Fig. 8 shows that atmospheric aerosols on
348 mainly consisted of six sources: industry, soil dust, secondary aerosols, sea salt, biomass burning, and
349 coal combustion/other sources, with 90% of the scaled residuals falling between -3 and +3; r^2=0.97. On
350 dust days, the sources of aerosols mainly included oil combustion, industry, soil dust, secondary
351 aerosols, and coal combustion/other sources. These values are compared in Table 7. The contribution of
352 soil dust increased from 23% to 36% on dust days relative to comparison days, consistent with the high
353 concentrations of TSPs and crustal metals observed on dust days. Liu et al. (2014) also found an even
354 larger increase in the contribution of dust aerosols to PM_{10}, i.e., 31%-40%, on dust days relative to
355 non-dust days. Accordingly, the contributions of local anthropogenic sources decreased on dust days,
356 especially those of secondary aerosols. The source profile for coal combustion in dust day samples
357 showed a high percentage of K^+, Cl^-, Ca, Mg, Co, Ni, As, Al and Fe, indicating a mixture of coal
358 combustion and other pollutants emitted along the transport path on dust days. The calculation results
359 also showed that the contribution of dust aerosol mass (the sum of nitrate and ammonium associated
360 with the dust source) to the total aerosol mass (the total nitrate and ammonium) greatly increased on
361 dust days.

362 **3.6 Dry deposition fluxes of TSP, particulate inorganic nitrogen and metals**

363 Dust events are known to increase the concentrations and deposition fluxes of aerosol particles
364 during long-range transport along the transport path. For example, Fu et al. (2014) found that the
365 long-range transported dust particles increased the dry deposition of PM_{10} in the Yangtze River Delta
366 region by a factor of approximately 20. In terms of atmospheric deposition in the oceans, some studies
367 reported enhancements in oceanic chlorophyll *a* following dust storm events (Tan and Wang, 2014;
368 Banerjee and Kumar, 2014). However, the deposition fluxes of dust varied greatly among different dust
369 storms, and only a few dust episodes were followed by an increase in oceanic chlorophyll *a* (Banerjee
370 and Kumar, 2014). In addition to those in high-nutrient and low-chlorophyll (HNLC) regions, the input
371 of nitrogen and other nutrients associated with dust deposition is expected to promote the growth of
372 phytoplankton. However, the extent canvary greatly depending on the nutrient limitation conditions in
373 the oceans. A similar principle holds for the occurrence or absence of algal blooms following dust
374 events. Thus, we calculated the dry deposition fluxes of aerosols particles, $N_{NH4+NO3}$ and metal

elements during dust and comparison periods using the measured component concentrations and modeled dry deposition velocities (Table 8). We then compared the dry deposition flux of TSP and $N_{NH4+NO3}$ with the previous observations in literature.

The dry deposition fluxes of atmospheric particulates increased on dust days relative to comparison days. All increases or decreases in this section reflected the value on dust days relative to comparison days, if not specified. For example, the dry deposition flux of TSP was only 2,800±700 mg/m^2/month on comparison days in the coastal region of the Yellow Sea. The particle fluxes varied over a wide range from 5,200 to 65,000 mg/m^2/month under different dust sampling days, with an average of 18,453 mg/m^2/month. However, the dry deposition fluxes of $N_{NH4+NO3}$- did not follow this pattern. In Category 1, the dry deposition fluxes of $N_{NH4+NO3}$ increased by 9-285%, corresponding to the increase in the TSP flux of 86-252% (Table S3). In Categories 2 and 3, the dry deposition fluxes of TSP increased by 126% to 2226% compared to that on comparison days. Except for ammonium in Category 3, the dry deposition fluxes of particulate $N_{NH4+NO3}$, however, decreased by 41% (on average). A larger relative decrease was found for the concentration of nitrate, i.e., decreases of 73% and 46% in Category 2 and 3, respectively. Note that the average ammonium deposition flux decreased by 47% in Category 2 but increase in Category 3.

The dry atmospheric deposition fluxes of Fe increased by a factor of 124-2370% on dust days. Atmospheric inputs of iron to the ocean have been proposed to enhance primary production in HNLC areas (Jickells et al., 2005). Moreover, except for Pb and Zn in Category 2, the dry deposition fluxes of Cu, Pb and Zn increased with those of nitrogen and iron on dust days. Trace metals were found to have a toxic effect on marine phytoplankton and inhibit their growth (Bielmyer et al., 2006; Echeveste et al., 2012). Liu et al. (2013) found that this inhibition coexisted with the promotion of some phytoplankton species in incubation experiments involving the addition of Asian dust samples in the southern Yellow Sea in the spring of 2011.

3.7 Potential impacts of nitrogen dry deposition flux associated with dust influenced byanthropogenic activity

Due to anthropogenic activity and economic development, inorganic nitrogen emissionsincreasedin China from 1980 to 2010 (Fig.S5). Accordingly, the $N_{NH4+NO3}$ dry deposition flux should have theoretically increased with the increase in inorganic nitrogen emissions. However, from the limited

404 data shown in Table 9, we did not find the expected increase in dry deposition flux of inorganic
405 nitrogen during the dust days. Considering the uncertainty in dry deposition velocity, we normalized
406 the dry deposition flux of $N_{NH4+NO3}$ using the concentration of nitrate and ammonium reported in the
407 literature and the recommended dry deposition velocity of 1 cm/s for nitrate and 0.1 m/s for ammonium
408 in coastal areas reported by Duce et al. (1991). We then found that dry deposition fluxes of $N_{NH4+NO3}$
409 over the Yellow Sea during the dust days increased greatly from 1999 to 2007. The fluxes of
410 $N_{NH4+NO3}$ in Qingdao, including during the dust days, varied narrowly in a range of 94.75-99.65 mg
411 N/m^2/month from 1997 to 2011 (Table 8). The complicated results may reflect the combined effects of
412 NOx and NH_3 emissions in northern China, the occurrence frequency and intensity of dust events and
413 metrological conditions affecting the transport pathways and moving speeds of dust air masses and
414 chemical reactions occurring therein. For example, dust events commonly exhibited a periodic
415 variation from 2000 to 2011 (Fig.S5).

416 **4 Conclusion**

417 The concentrations of nitrate and ammonium in TSP samples varied greatly from event to event on
418 dust days. Relative to non-dust day samples, the concentrations were both higher in some cases and
419 lower in others. The observed ammonium in dust day samples was explained by ammonium salt
420 aerosols co-existing externally with dust aerosols or the residual of incomplete reactions between
421 ammonium salts and carbonate salts. NO_3^- in the dust day samples was partially related to mixing and
422 reactions between anthropogenic air pollutants and dust particles during the transport from the source
423 zone to the reception site. However, this process was generally much less effective and led to a sharp
424 decrease in nitrate in Category 2 TSP samples. The external co-existence of ammonium salt aerosols
425 with dust aerosols and the extent of the reactions between ammonium salts and carbonate salts were
426 apparently associated with the transport pathway, moving speeds and metrological conditions, among
427 other factors.

428 Due to a sharp increase in dust loads on dust days, the contribution of soil dust to the total aerosol
429 mass was higher on dust days than on comparison days, while the contributions from local
430 anthropogenic sources were accordingly lower.

431 Overall, this study strongly suggested that atmospheric deposition of $N_{NH4+NO3-}$ on dust days varied

greatly and that no simple linear increase existed with increasing dust load. More observations at various locations are needed to obtain a statistical relationship between dust events and atmospheric deposition of $N_{NH4+NO3-}$. A simple assumption of a linear increase in $N_{NH4+NO3-}$ with increasing dust load, like that in the literature, could lead to considerable overestimation of the dry deposition flux of nutrients into the oceans and the consequent primary production associated with dust events.

*Acknowledgments.*This work was supported by the Department of Science and Technology of the P. R. China through the State Key Basic Research & Development Program under Grant No. 2014CB953701 and the National Natural Science Foundation of China (No. 41375143). We thank Prof. Yaqiang Wang and Jinhui Shi for the valuable discussion regarding this research. We also express our appreciation to Tianran Zhang for help with sand sampling and Qiang Zhang for data collection.

References

Banerjee, P., and Kumar,P. S.: Dust-induced episodic phytoplankton blooms in the Arabian Sea during winter monsoon, J. Geophys.Res-Oceans., 119, 7123-7138, 2014.

Bielmyer, G. K., Grosell, M., and Brix, K. V.: Toxicity of silver, zinc, copper, and nickel to the copepod Acartiatonsa exposed via a phytoplankton diet, Environ. Sci. technol., 40, 2063-2068, 2006.

Chen, D., Liu, Z. Q., Fast, J., and Ban, J. M.: Simulations of sulfate–nitrate–ammonium (SNA) aerosols during the extreme haze events over northern china in october 2014, Atmos. Chem. Phys., 16, 10707-10724, 2016.

CMA: Regulations of Surface Meteorological Observation, China Meteorological Press, Beijing, 154–156, 2004.

CMA: Sand-dust weather almanac 2011, China Meteorological Press, Beijing, 36-53, 2013.

Cui, W. L., Guo, R., and Zhang, H.: The Long-range Transport of Dust from MongoliaGobi to the Yangtze River Basin and itsMixing with Pollutant Aerosols, Journal of Fudan University (Natural Science), 48, 585-592, 2009a.

Cui, W. L.: Chemical transformation of dust components and mixing mechanisms of dust with pollution aerosols during the long range transport from north to south China, M.S. thesis, Department of Environmental Science and Engineering, Fudan University, China, 38 pp., 2009b.

Dai, Y.J.: Vertical distribution of characteristics of dust aerosols in the near-surface in hinterland of Taklimakan Desert, M.S. thesis, College of Resources and Environmental Science, Xinjiang University, China, 26 pp., 2016.

Duce, R. A., LaRoche, J.,Altieri, K., Arrigo, K. R., Baker, A. R., Capone, D. G., Cornell, S.,Dentener, F., Galloway, J., Ganeshram,R. S.,Geider, R. J., JickellsT., Kuypers, M. M.,Langlois, R., Liss, P. S.,Liu, S. M.,Middelburg, J. J.,Moore, C. M., Nickovic, S.,Oschlies, A., Pedersen, T., Prospero, J., Schlitzer, R., Seitzinger, S., Sorensen, L. L.,Uematsu, M., Ulloa, O., Voss, M., Ward, B., and Zamora, L.: Impacts of atmospheric anthropogenic nitrogen on the open ocean, Science, 320, 893-897, 2008.

Duce, R. A., Liss, P. S., Merrill, J. T., Atlas, E. L., Buat-Menard, P., Hicks, B. B., Miller, J. M.,

Prospero, J. M., Arimoto, R., Church, T. M., Ellis, W., Galloway, J. N., Hansen, L., Jickells, T. D., Knap, A. H., Reinhardt, K. H., Schneider, B., Soudine, A., Tokos, J. J., Tsunogai, S., Wollast, R., and Zhou, M. Y.: The atmospheric input of trace species to the world ocean, Global. Biogeochem.Cy., 5, 193-259, 1991.

Echeveste, P., Agustí, S., and Tovar-Sánchez, A.: Toxic thresholds of cadmium and lead to oceanic phytoplankton: cell size and ocean basin-dependent effects, Environ.Toxicol.Chem., 31, 1887–1894, 2012.

Fitzgerald, E., Ault, A. P., Zauscher, M. D., Mayol-Bracero, O. L., and Prather, K. A.: Comparison of the mixing state of long-range transported Asian and African mineral dust, Atmos. Environ., 115, 19-25, 2015.

Fu, X., Wang, S. X., Cheng, Z., Xing, J., Zhao, B., Wang, J. D., and Hao, J. M.: Source, transport and impacts of a heavy dust event in the Yangtze River Delta, China, in 2011, Atmos. Chem. Phys., 14, 1239-1254, 2014.

Grice, S., Stedman, J., Kent, A., Hobson, M., Norris, J., Abbott, J., and Cooke, S.:Recent trends and projections of primary NO_2emissions in Europe, Atmos. Environ., 43, 2154-2167, 2009.

Guo, C., Yu, J., Ho, T. Y., Wang, L., Song, S., Kong, L., and Liu, H.: Dynamics of phytoplankton community structure in the South China Sea in response to the East Asian aerosol input, Biogeosciences, 9, 1519-1536, 2012.

Han, X., Ge, C., Tao, J. H., Zhang, M. G., and Zhang, R. J.: Air Quality Modeling for of a Strong Dust Event in East Asia in March 2010, Aerosol. Air. Qual. Res., 12, 615-628, 2012.

Jickells, T. D., An, Z. S., Andersen, K. K., Baker, A. R., Bergametti, G., Brooks, N., Cao, J. J., Boyd, P. W., Duce, R. A., Hunter, K., Kawahata, H., Kubilay, N., laRoche, J.,Liss, P. S.,Mahowald, N., Prospero, J. M., Ridgwell, A. J., Tegen, I., and Torres, R.: Global iron connections between desert dust, ocean biogeochemistry, and climate, Science, 308, 67-71, 2005.

Kang, E., Han, J., Lee, M., Lee, G., and Kim, J. C.: Chemical characteristics of size-resolved aerosols from Asian dust and haze episode in Seoul Metropolitan City, Atmos. Res., 127, 34-46, 2013.

Li, W. J., Shao, L. Y., Shi, Z. B., Chen, J. M., Yang, L. X., Yuan, Q., Yan, C., Zhang, X. Y., Wang, Y. Q., Sun, J. Y., Zhang, Y, M., Shen, X. J., Wang, Z. F., and Wang, W. X.: Mixing state and hygroscopicity of dust and haze particles before leaving Asian continent, J.Geophys.Res-Atmos, 119, 1044–1059, 2014.

Lin, X. H., Liu, C. L., and Zhang, H.: Determination of Metal Elements in Aerosol by ICP-AES, Rock & Mineral Analysis, 17, 143-146, 1998.

Liu, L., Zhang, X. Y., Xu W., Liu, X. J., Li, Y., Lu, X. H., Zhang, Y. H., and Zhang, W. T.: Temporal characteristics of atmospheric ammonia and nitrogen dioxide over China based on emission data, satellite observations and atmospheric transport modeling since 1980, Atmos. Chem. Phys., 106, 1-32, 2017.

Liu, Q. Y., and Bei, Y. L.: Impacts of crystal metal on secondary aliphatic amine aerosol formation during dust storm episodes in Beijing, Atmos. Environ., 128, 227-334, 2016.

Liu, Q. Y., Liu, Y. J., Yin, J. X., Zhang, M. G., and Zhang, T. T.: Chemical characteristics and source apportionment of PM 10 during Asian dust storm and non-dust storm days in Beijing, Atmos. Environ., 91, 85-94, 2014.

Liu, X. H., Zhang, Y., Cheng, S. H., Xing, J., Zhang, Q.,Streets, D. G., Jang, C., Wang, W. X., and Hao, J. M.: Understanding of regional air pollution over China using CMAQ, part I performance evaluation and seasonal variation, Atmos. Environ., 44, 2415-2426, 2010a.

513 Liu, X. H., Zhang, Y., Xing, J., Zhang, Q.,Wang, K., Streets, D. G., Jang, C.,Wang, W. X., and Hao, J.
514 M.: Understanding of regional air pollution over China using CMAQ, part II. Process analysis and
515 sensitivity of ozone and particulate matter to precursor emissions, Atmos. Environ., 44, 3719-3727,
516 2010b.
517 Liu, Y., Zhang, T. R., Shi, J. H., Gao, H. W., and Yao, X. H.: Responses of chlorophyll a to added
518 nutrients, Asian dust, and rainwater in an oligotrophic zone of the Yellow Sea: Implications for
519 promotion and inhibition effects in an incubation experiment, J. Geophys.Res-Biogeo, 118,
520 1763-1772, 2013.
521 Ma, Q. X., Liu, Y. C., Liu, C., Ma, J. Z., and He, H.: A case study of Asian dust storm particles:
522 Chemical composition, reactivity to SO2 and hygroscopic properties, J. Environ. Sci., 24, 62-71,
523 2012.
524 Mori, I., Nishikawa, M., Tanimura, T., and Quan, H.: Change in size distribution and chemical
525 composition of kosa (Asian dust) aerosol during long-range transport, Atmos. Environ., 37,
526 4253-4263, 2003.
527 Niu, S. J., and Zhang, C. C.: Researches on Sand Aerosol Chemical Composition and Enrichment
528 Factor in the Spring at Helan Mountain Area, Journal of Desert Research, 20, 264-268, 2000.
529 Ohara, T., Akimoto, H., Kurokawa, J., Horii, N., Yamaji, K., Yan, X., and Hayasaka, T.: An Asian
530 emission inventory of anthropogenic emission sources for the period 1980–2020, Atmos. Chem.
531 Phys., 7, 4419-4444, 2007.
532 Paatero, P., and Tapper, U.: Analysis of different modes of factor analysis as least squares fit problems,
533 Chemometr. Intell.Lab., 18, 183-194, 1993.
534 Paatero, P.: Least squares formulation of robust non-negative factor analysis, Chemometr. Intell.Lab.,
535 37, 23-35, 1997.
536 Penrod, A., Zhang, Y., Wang, K., Wu, S. Y. and Leung, L. R.: Impacts of future climate and emission
537 changes on U.S. air quality, Atmos. Environ., 89, 533-547, 2014.
538 Qi, J. H., Gao, H. W., Yu, L. M., and Qiao, J. J.: Distribution of inorganic nitrogen-containing species
539 in atmospheric particles from an island in the Yellow Sea, Atmos. Res., 101, 938-955, 2011.
540 Qi, J. H., Li, P. L., Li, X. G., Feng, L. J., and Zhang, M. P.: Estimation of dry deposition fluxes of
541 particulate species to the water surface in the Qingdao area, using a model and surrogate surfaces,
542 Atmos. Environ., 39, 2081-2088, 2005.
543 Qi, J. H., Shi, J. H., Gao, H. W., and Sun, Z.: Atmospheric dry and wet deposition of nitrogen species
544 and its implication for primary productivity in coastal region of the Yellow Sea, China, Atmos.
545 Environ.,81, 600-608, 2013.
546 Sheng, Y., Yang, S., Han, Y., Zheng, Q., and Fang, X.: The concentrations and sources of nitrate in
547 aerosol over Dolmud, Qinghai, China, Journal of Desert Research,36, 792-797, 2016.
548 Shi, J. H., Gao, H. W., Zhang, J., Tan, S. C., Ren, J. L., Liu, C. G., Liu, Y., and Yao, X. H.: Examination
549 of causative link between a spring bloom and dry/wet deposition of Asian dust in the Yellow Sea,
550 China, J.Geophys.Res-Atmos., 117, 127-135, 2012.
551 Shi, J. H., Zhang, J., Gao, H. W., Tan, S. C., Yao, X. H., and Ren, J. L.: Concentration, solubility and
552 deposition flux of atmospheric particulate nutrients over the Yellow Sea, Deep-sea. Res. Pt. II, 97,
553 43–50, 2013.
554 Skjøth C. A., and Hertel, O.: Ammonia Emissions in Europe, Urban Air Quality in Europe, Springer
555 Berlin Heidelberg, The Handbook of Environmental Chemistry, Germany, 163 pp., 2013.
556 Tan, S. C., and Wang, H.: The transport and deposition of dust and its impact on phytoplankton growth

557 in the Yellow Sea, Atmos. Environ., 99, 491-499, 2014.
558 Taylor, S. R.: Abundance of chemical elements in the continental crust: a new
559 table,Geochim.Cosmochim.Ac., 28, 1273-1285, 1964.
560 U. S., EPA.: Method 1631, Revision E: Mercury in water by oxidation, purge and trap, and cold vapor
561 atomic fluorescence spectrometry, US Environmental Protection Agency Washington, DC, 2002.
562 Uno, I., Carmichael, G. R., Streets, D. G., Tang, Y., Yienger, J. J., Satake, S., Wang, Z., Woo, J. H.,
563 Guttikunda, S., Uematsu, M., Matsumoto, K., Tanimoto, H., Yoshioka, K., and Iida, T.: Regional
564 chemical weather forecasting system CFORS: Model descriptions and analysis of surface
565 observations at Japanese island stations during the ACE-Asia experiment, J. Geophys. Res-Atmos.,
566 108, 1147-1164, 2003.
567 Walker, J. M., Philip, S., Martin, R. V., and Seinfeld, J. H.: Simulation of nitrate, sulfate, and
568 ammonium aerosols over the United States, Atmos. Chem. Phys., 12, 11213-11227, 2012.
569 Wang, L., Du, H. H., Chen, J. M., Zhang, M., Huang, X. Y., Tan, H. B., Kong, L. D., and Geng, F. H.:
570 Consecutive transport of anthropogenic air masses and dust storm plume: Two case events at
571 Shanghai, China, Atmos. Res., 127, 22-33, 2013.
572 Wang, Q. Z., Zhuang, G. S., Huang, K., Liu, T. N., Lin, Y. F., Deng, C. R., Fu, Q. Y., Fu, J. S., Chen, J.
573 K., Zhang, W. J., and Yiming, M.: Evolution of particulate sulfate and nitrate along the Asian dust
574 pathway: Secondary transformation and primary pollutants via long-range transport, Atmos. Res.,
575 169, 86-95, 2016.
576 Wang, Q. Z., Zhuang, G. S., Li, J., Huang, K., Zhang, R., Jiang, Y. L., Lin, Y. F., and Fu, J. S.: Mixing
577 of dust with pollution on the transport path of Asian dust — Revealed from the aerosol over Yulin,
578 the north edge of Loess Plateau, Sci. Total.Environ.,409, 573–581, 2011.
579 Wang, Y. Q., Zhang, X. Y., and Draxler, R. R.: TrajStat: GIS-based software that uses various trajectory
580 statistical analysis methods to identify potential sources from long-term air pollution measurement
581 data, Environ. Modell.Softw., 24, 938-939, 2009.
582 Wang, Y. Q., Zhang, X. Y., Gong, S. L., Zhou, C. H., Hu, X. Q., Liu, H. L., Niu, T., and Yang, Y. Q.:
583 Surface observation of sand and dust storm in East Asia and its application in CUACE/Dust, Atmos.
584 Chem. Phys., 8, 545–553, 2008.
585 Wang, Z., Pan, X. L., Uno, I., Li, J., Wang, Z. F., Chen, X. S., Fu, P. Q., Yang, T., Kobayashi, H.,
586 Shimizu, A., Sugimoto, N., and Yamamoto, S.: Significant impacts of heterogeneous reactions on the
587 chemical composition and mixing state of dust particles: A case study during dust events over
588 northern China, Atmos. Environ., 159, 83-91, 2017 .
589 Williams, R. W.: A model for the dry deposition of particles to natural water surface. Atmos. Environ.,
590 16, 1933-1938, 1982.
591 Wu, F., Zhang, D. Z., Cao, J. J., Guo, X., Xia, Y., Zhang, T., Lu, H., and Cheng, Y.: Limited production
592 of sulfate and nitrate on front-associated dust storm particles moving from desert to distant populated
593 areas in northwestern China, Atmos. Chem. Phys.,853, 1-22, 2016.
594 Xin, W. C., Lin, X. H., and Xu, L.: ICP-MS Determination of 34 Trace Elements in Marine Sediments,
595 Physical Testing and Chemical Analysis (Part B: Chemical Analysis), 4, 29, 2012.
596 Xu, J. Z., Wang, Z. B., Yu, G. M., Qin, X., Ren, J. W., and Qin, D. H.: Characteristics of water soluble
597 ionic species in fine particles from a high altitude site on the northern boundary of Tibetan Plateau:
598 Mixture of mineral dust and anthropogenic aerosol, Atmos. Res., 143, 43-56, 2014.
599 Yang, D. Z., Wang, C., Wen, Y. P., Yu, X. L., and Xiu, X. B.: Ananalysis of Two Sand Storms In Spring
600 1990, Quarterly Journal of Applied Meteorology, 6, 18-26, 1995.

Yang, D. Z., Yan, P., and Xu, X. D.: Characteristics of aerosols under dust and sand weather in Beijing, Quarterly Journal of Applied Meteorology, 1, 185-194, 2002.

Yao, X. H., and Zhang, L.:Supermicron modes of ammonium ions related to fog in rural atmosphere, Atmos. Chem. Phys., 12, 11165-11178, 2012.

Yao, X. H., Lau, A. S., Fang, M., Chan, C., and Hu, M.: Size Distributions and Formation of Ionic Species in Atmospheric Particulate Pollutants in Beijing, China: 1—Inorganic Ions. Atmos. Environ., 37, 2991-3000, 2003.

Zhang, D., and Iwasaka, Y.: Nitrate and sulfate in individual Asian dust-storm particles inBeijing, China in spring of 1995 and 1996, Atmos. Environ.,33, 3213-3223, 1999.

Zhang, G. S., Zhang, J., and Liu, S. M.: Characterization of nutrients in the atmospheric wetand dry deposition observed at the two monitoring sitesover Yellow Sea and East China Sea, J. Atmos. Chem., 57, 42-57, 2007.

Zhang, J., Zhang, G. S., Bi, Y. F., and Liu, S. M.: Nitrogen species in rainwater and aerosols of the Yellow and East China seas: Effects of the East Asian monsoon and anthropogenic emissions and relevance for the NW Pacific Ocean, Global Biogeochem. Cy., 25, 113-120, 2011.

Zhang, K., and Gao, H. W.: The characteristics of Asian-dust storms during 2000–2002: From the source to the sea, Atmos. Environ., 41, 9136-9145, 2007.

Zhang, Q., Streets, D. G., Carmichael, G. R., He, K. B., Huo, H., Kannari, A., Klimont,Z., Park, I. S., Reddy, S., Fu, J. S., Chen, D.,Duan, L., Lei, Y., Wang, L. T., and Yao, Z. L.: Asian emissions in 2006 for the NASA INTEX-B mission. Atmos. Chem. Phys., 9, 5131-5153, 2009.

Zhang, W. J., Zhuang, G. S., Huang, K., Li, J., Zhang, R., Wang, Q. Z., Sun, Y. L., Fu, J. S., Chen, Y., and Xu, D. Q.: Mixing and transformation of Asian dust with pollution in the two dust storms over the northern China in 2006, Atmos. Environ., 44, 3394-3403, 2010a.

Zhang, Y., Yu, Q., Ma, W. C., and Chen, L. M.: Atmospheric deposition of inorganic nitrogen to the eastern China seas and its implications to marine biogeochemistry, J.Geophys. Res-Atmos, 115, 3421-3423, 2010b.

645 **Table 1**. Sampling information for the aerosol samples collected at the Baguanshan site in thecoastal
646 region of the Yellow Sea.

Sampling Year	Sample category	Sampling number	Sampling time	Weather characteristics
2008	Samples on dust days	20080301	From 13:22 a.m. to 17:22 p.m. on Mar. 1st	Floating dust[a]
		20080315	From 13:21 a.m. to 17:21 p.m.on Mar. 15th	Floating dust
		20080425	From 13:14 a.m. to 17:14 p.m. on Apr. 25th	Floating dust
		20080528	From 11:38 a.m. to 15:38 p.m. on May 28th	Floating dust
		20080529	From 10:15 a.m.to 12:15 p. m. on May 29th[b]	Floating dust
	Samples on non-dust days	20080316	From 13:00 a.m. to 17:00 p.m. on Mar. 16th	Sunny day
		20080424	From 13:00 a.m. to 17:00 p.m. on Apr. 24th	Sunny day
		20080522	From 13:00 a.m. to 17:00 p.m. on May 22nd	Cloudy day with mist
2009	Samples on dust days	20090316	From 8:25 a.m. to 12:25 p.m. on Mar. 16th	Floating dust
	Samples on non-dust days	20090306	From 13:00 a.m.to 17:00 p.m. on Mar. 6th	Sunny day
2010	Samples on dust days	20100315	From 11:30 a.m.to 15:30 p.m. on Mar. 16th	Mist after floating dust
		20100320	From 10:30 a.m. to 14:30 p.m. on Mar. 20th	Floating dust
		20100321	From 10:30 a.m. to 14:30 p.m. on Mar. 21st	Floating dust
	Samples on non-dust days	20100324	From 11:30 a.m. to 15:30 p.m. on Mar. 24th	Sunny day
2011	Samples on dust days	20110319	From 12:00 a.m. to 16:00 p.m. on Mar. 19th	Floating dust
		20110415	From 12:00 a.m. to 16:00 p.m. on Apr. 15th	Floating dust
		20110418	From 12:25 a.m. to 16:25 p.m. on Apr. 18th	Floating dust[c]
		20110501	From 12:10 a.m. to 16:10 p.m. on May 1st	Floating dust
		20110502	From 16:00 a.m. to 20:00 p.m. on May 2nd	Floating dust
	Samples on non-dust days	20110308	From 12:00 a.m. to 16:00 p.m. on Mar. 8th	Sunny day

	20110416	From 12:00 a.m. to 16:00 p.m. on Apr. 16th	Sunny day
	20110523	From 12:00 a.m. to 16:00 p.m. on May 23rd	Sunny day

[a]Note that one exterior dust sample was collected on March 1 when no dust was recorded by the MICAPS. However, the MICAPSinformation indeed showed dust events in China on March 1. The modeled spatial distribution of thePM_{10} mass concentration for this dust event on March 1 implies that the sample should be classified as adust sample. The supporting figureisFig. S1.

[b]The sampling duration was reduced to only 2 hrs because of extremely high particle loads.

[c]Note that one exterior dust sample was collected on April 18when no dust was recorded by the MICAPS. However, blowing dust occurred and was recorded on April 17 by the Sand-dust weather almanac 2011 (CMA, 2013). The modeled spatial distribution of the PM_{10} mass concentration for this dust eventon April 18implies that the sample should be classified as adust sample. The supporting figure is Fig. S2.

687 **Table 2.** Detection limits, precisions and recoveries of water-soluble ions and metal elements.

Component	Measurement method	Detection limit ($\mu g \cdot L^{-1}$)	Precision (RSD%)	Recovery (%)
NO_3^-	IC	2.72	1.54	97
SO_4^{2-}		1.62	1.55	98
NH_4^+		0.4	1.10	97
Ca^{2+}		0.44	0.79	94
Cu	ICP-MS (Xin et al., 2012)	0.006	4.0	106
Zn		0.009	2.5	102
Cr		0.004	3.0	95
Sc		0.002	2.4	97
Pb		0.008	3.9	104
Al	ICP-AES (Lin et al., 1998)	7.9	0.6	103
Ca		5.0	1.2	99
Fe		2.6	0.7	104
Na		3.0	0.6	99
Mg		0.6	0.6	105
Hg	CVAFS	0.0001	6.6	105
As	CVAFS	0.1	5.0	98

688
689
690
691
692
693
694
695
696
697
698
699
700
701
702
703
704
705
706
707
708
709
710
711
712

713 **Table 3.** Theaverage concentrations and EFs of metal elements on dust and non-dust days.

Element	Concentration (ng/m^3)		EF*	
	Non-dust days	Dust days	Non-dust days	Dust days
Sc	1.11	13.90	-	-
Al	8.53×10^3	6.86×10^4	3.8	1.4
Fe	4.91×10^3	3.88×10^4	3.	1.2
Ca	1.05×10^4	4.29×10^4	14.0	2.1
Mg	1.62×10^3	1.58×10^4	3.5	1.1
Cu	50.2	124.5	36.3	6.1
Pb	127.9	221.0	389.4	56.1
Zn	340.0	457.7	248.9	20.6
Cr	33.8	244.0	44.0	11.1
Hg	0.26	0.36	176.0	13.8
As	25.5	27.4	707.2	43.9

714 *EF valuesless than 10 indicate that the studied element is derived mainly from crustal
715 sources,whereasEF valuesmuch higher than 10 indicatea anthropogenic source.
716
717
718
719
720
721
722
723
724
725
726
727
728
729
730
731
732
733
734
735
736
737
738
739
740
741
742
743

744 **Table 4.** Average concentrations of inorganic nitrogen (DIN), TSP, NOx, relative humidity (RH) and
745 air temperature for each aerosol samplecategoryin Qingdao.

	Sample number	TSP $\mu g \cdot m^{-3}$	NO_3^- $\mu g \cdot m^{-3}$	NH_4^+ $\mu g \cdot m^{-3}$	RH %	T °C	NOx $\mu g \cdot m^{-3}$	Summary
Category 1	20080301	527	20.5	12.7	57	7.0	36	DIN concentrationon dust days higher than that on non-dustdays
	20080315	410	19. 5	29.9	62	11.0	59	
	20090316	688	15.9	17.2	27	16.0	75	
	20100321	519	16.5	9.4	51	8.8	76	
	20110502	810	21.0	11.0	49	17.7	62	
Category 2	20080425	622	6.8	2.0	30	18.0	40	DIN concentrationon dust days lower than that on non-dust days
	20080528	2579	9.2	2.7	17	27.0	34	
	20080529	2314	17.5	4.8	60	20.0	29	
	20110319	939	12.3	9.4	16	12.6	93	
	20110501	502	4.5	5.3	23	21.6	66	
Category 3	20100315	501	5.4	4.3	30	7.2	73	NO_3^- concentration on dust days lower than that on non-dust days;NH_4^+close to that on non-dust days
	20100320	3857	5.5	3.4	35	10.6	92	
	20110418	558	3.8	6.6	33	12.6	47	
Non-dust[a]	20080316	225	12.6	8.4	28	11.0	60	
	20080424	137	21.7	7.2	49	18.0	53	
	20080522	206	27.4	16.6	78	20.0	60	
	20090306	94	2.9	3.0	29	7.00	51	
	20100324	275	7.2	2.4	23	9.0	82	
	20110308	194	13.0	13.1	20	11.5	111	
	20110416	252	5.6	5.4	26	14.1	55	
	20110523	224	15.2	10.2	42	20.6	49	

746 [a]For the corresponding non-dustday for each dust event, see Table 1.
747
748
749
750
751

752 **Table 5.** Comparison of the inorganic nitrogen (DIN) content in sandand aerosol particles on dust days
753 or close to the dust source region (unit: μg/g)

Sands sampled in dust source regions			Aerosols in or close to dust source region on dust days			Aerosols in the coastal region of the Yellow Sea	
Study region and data source	Relative concentration[a]		Study region and data source	Relative concentration[a]			
	NO_3^-	NH_4^+		NO_3^-	NH_4^+	NO_3^-	NH_4^+
Zhurihe (This study)	25.46± 22.87	4.21± 1.03	Duolun (Cui, 2009)	1200	900	Non-dust: 28,200±24,819	Non-dust: 24,063±21,515
AlxaLeft Banner, Inner Mongolia (NiuandZhang, 2000)	62.1±7.4	79.1±1.1	AlxaRightBanner, Inner Mongolia (NiuandZhang, 2000)	1975[b]	4091[b]	Category 1: 34,892±9570	Category 1: 22,571±7,016
Yanchi, Ningxia (NiuandZhang, 2000)	46.4±2.2	80.9±1.3	Hinterland of theTaklimakan Desert, Xinjiang (Dai et al., 2016)	142-233	2-15	Category 2: 5,542±5,117	Category 2: 4,758±5,698
			Average of SonidYouqi, Huade (Inner Mongolia), Zhangbei (Hebei) (Mori et al., 2003)	253	710	Category 3: 6,359±4,697	Category 3: 7,059±5,591
			Yulin, the north edge of Loess Plateau (Wang et al., 2011)	216.4	80.6		
			Golmud, Qinghai(Sheng et al., 2016)	892.9	-[c]		
			Hohhot, Inner Mongolia (Yang et al., 1995)	588.1	No data		

754 [a]Relative concentration of DIN per aerosol particle mass

755 [b] Samples collected on a floating dust day (Horizontalvisibility less than 10000 m and very low wind speed)

756 [c] The ammonium concentration was lower than the detection limit of the analytical instrument.

757

758

759

760

761

Table 6. Concentrations of TSP, NO_3^-, and NH_4^+; transport speed; transport distance over the sea; transport distance; air temperature; RH; average mixed layer during transport and transport time in polluted region for atmospheric aerosol samples on dust days.

Group	Sample number	TSP (μg/m^3)	NO_3^- (μg/g)	NH_4^+ (μg/g)	Speed (km/h)	Distance over the sea (km)	Transport altitude (m)	Mixed layer depth (m)	Residence time[a] (h)	T[b] (℃)	RH (%)
Category 1 IN>ND	080301	527	38,984	24,107	40.1	0	1,160±702	864±745	39	-2.9±11.7	29±10
	080315	410	47,611	34,130	79.1	0	4,921±1,870	950±525	13	-32.5± 16.4	34±16
	090316	688	23,050	25,012	86.2	0	3,739±1083	702±665	11	-19.1±11.7	42±17
	100321	519	31,741	18,155	87.2	0	3,407±1,249	1,113±760	19	-23.0±13.6	42±22
	110502	810	25,995	13,632	30.2	177	3,666±1,371	747±957	26	-13.2±15.8	31±13
Category 2 IN<ND	080425	256	4,089	372	29.6	0	887±656	1,161±1,040	10	-2.7±6.1	66±13
	080528	2579	232	72	88.2	244	4,336±1461	1,064±830	8	-15.5±13.6	31±16
	080529	2314	26	166	63.7	94	2,148±1,725	1,194±816	43	3.6±18.4	25±17
	110319	939	13,088	10,067	70.6	132	4,271±1867	790±719	27	-26.3±20.0	48±32
	110501	502	8,924	10,631	35.1	252	3,212±810	916±1,114	5	-13.4±8.5	39±13
Category 3 NO_3^-<ND NH_4^+≅ND	100315	501	10,767	8,515	57.3	0	5,009±1410	1,110±365	7	-40.4±13.3	45±29
	100320	3857	1,418	884	76.9	0	1,284±401	525±371	10	-12.2±6.3	61±16
	110418	558	6,891	11,778	35.6	931	1,344±780	695±672	2	-0.1±8.2	52±28

Table 7. Sources and source contributions (expressed in%) calculated for aerosolsamples collected during dust and non-dust events

Dust event		Comparison days	
Source	% of TSP	Source	% of TSP
Soil dust	36	Soil dust	23
Industrial	21	Industrial	24
Secondary aerosol	6	Secondary aerosol	23
Oil combustion	6	Biomass burning	16
Coal combustion and other uncertain sources	31	Coal combustion	5
		Sea salt	9

Table 8. Dry deposition of TSP (mg/m^2/month), particulate inorganic nitrogen (mg N/m^2/month) and some toxic trace metals (mg/m^2/month) on dust and non-dust days.

	Dry deposition flux							
	TSP	NO_3^--N	NH_4^+-N	$N_{NH4+NO3}$-	Fe	Cu	Pb	Zn
Category 1[a]	8,000±1800	65±9	24±14	90±17	533±179	2±0.3	0.3±0.3	6±2
Category 2[a]	18000±11,000	13±18	8±4	21±22	1300±1000	3±2	0.08±0.04	4±1
Category 3[a]	29,000±31,000	26±6	17±8	42±12	2100±2200	6±1	0.20±0.02	5±3
Non-dust	2,800±700	48±33	15±8	63±39	190±110	1±1	0.09±0.1	5±4

[a]For the characterization of$N_{NH4+NO3}$- concentration and sample information of the category, see in Table 3.

847 **Table 9.** Comparison of dry deposition flux and normalized flux of TSP (mg/m^2/month) and $N_{NH4++NO3}$-
848 (mg N/m^2/month) with observations from other studies(mg N/m^2/month)

Source	Year	Area		TSP	$N_{NH4++NO3}$-	Normalized average flux of $N_{NH4++NO3}$-[a]
This work	2008-2011	Qingdao, coastal region of the Yellow Sea	Non-dust day	2,800±700	63±39	93.90
			Dust day	10,138±15,940	58±36	101.39
			Average of dust and non-dust			97.64
Qi et al., 2013	2005-2006	Qingdao, coastal region of the Yellow Sea	Average of nine months samples	159.2 - 3,172.9	1.8-24.5	94.75
Zhang et al., 2011	1997-2005	Qingdao	Average of annual samples		132	99.65
Zhang et al., 2007	1999-2003	The Yellow Sea			11.43	9.91
Shi et al., 2013	2007	The Yellow Sea	Non-dust day		19.2	132.17
			Dust day		104.4	227.07
			Average of dust and non-dust			179.62

849 [a] The calculation method of normalized flux of $N_{NH4++NO3}$- was discussed in section 3.7.
850
851
852
853
854
855
856

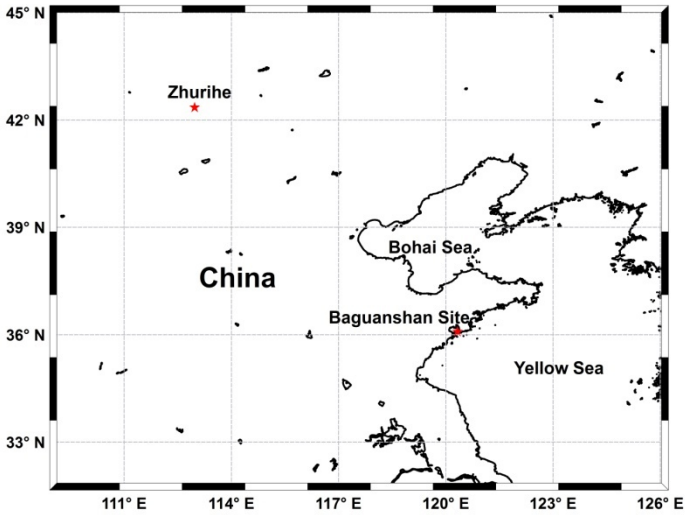

Figure 1. Location of the aerosol and dust sampling sites.

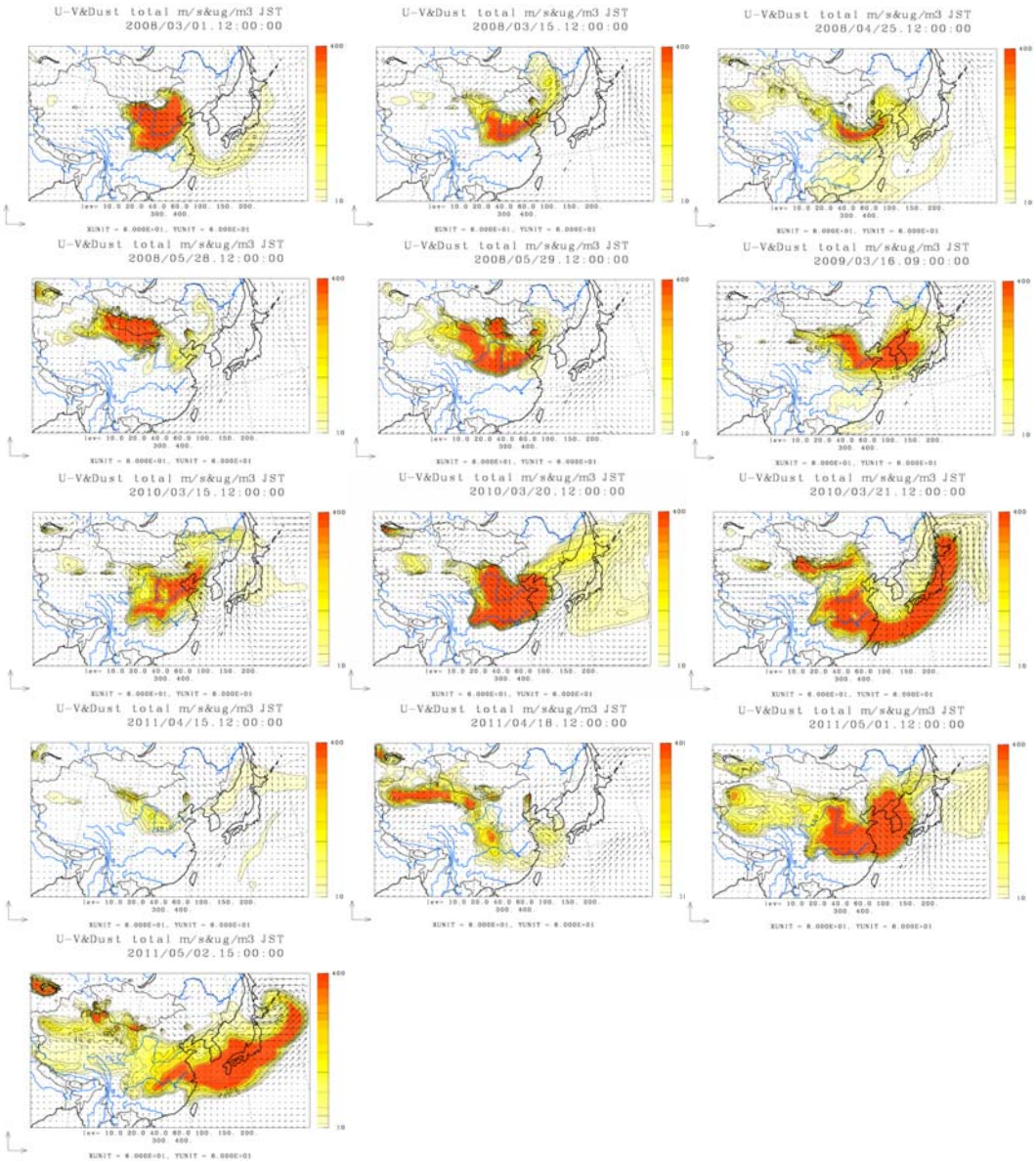

Figure 2. Modeleddust concentrations over East Asia by CFORSmodel during each dust sampling day from 2008 to 2011(http://www-cfors.nies.go.jp/). (The figures showthe modeled dust concentration inthe middle of each sampling duration). Nodata are available forMar.19, 2011,because of the earthquake in Japan.Hourly PM10 concentrationsweremodeled by the WRF-CMAQ model for eachsampling day,and the resultsareshownin Fig. S3.

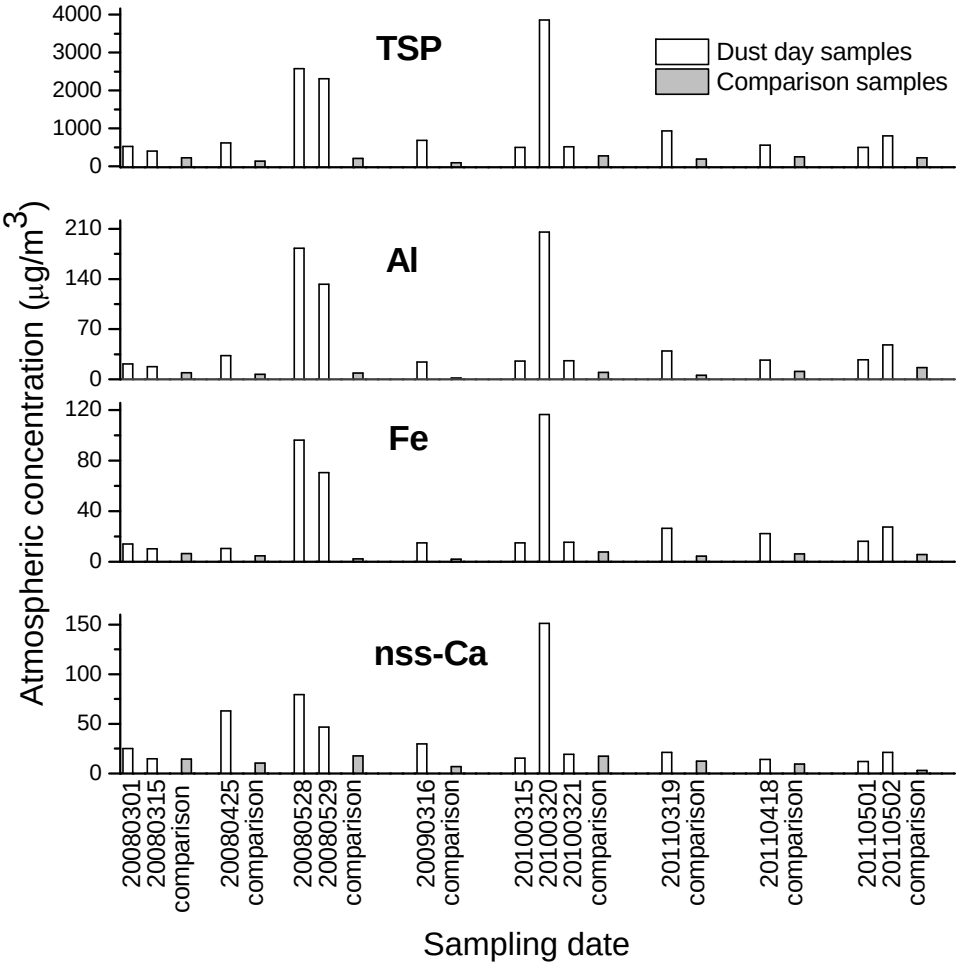

Figure 3. Mass concentrations of TSP, Al, Fe and nss-Ca in aerosol samples collected at the Baguanshan site on dust and comparison days from2008-2011.

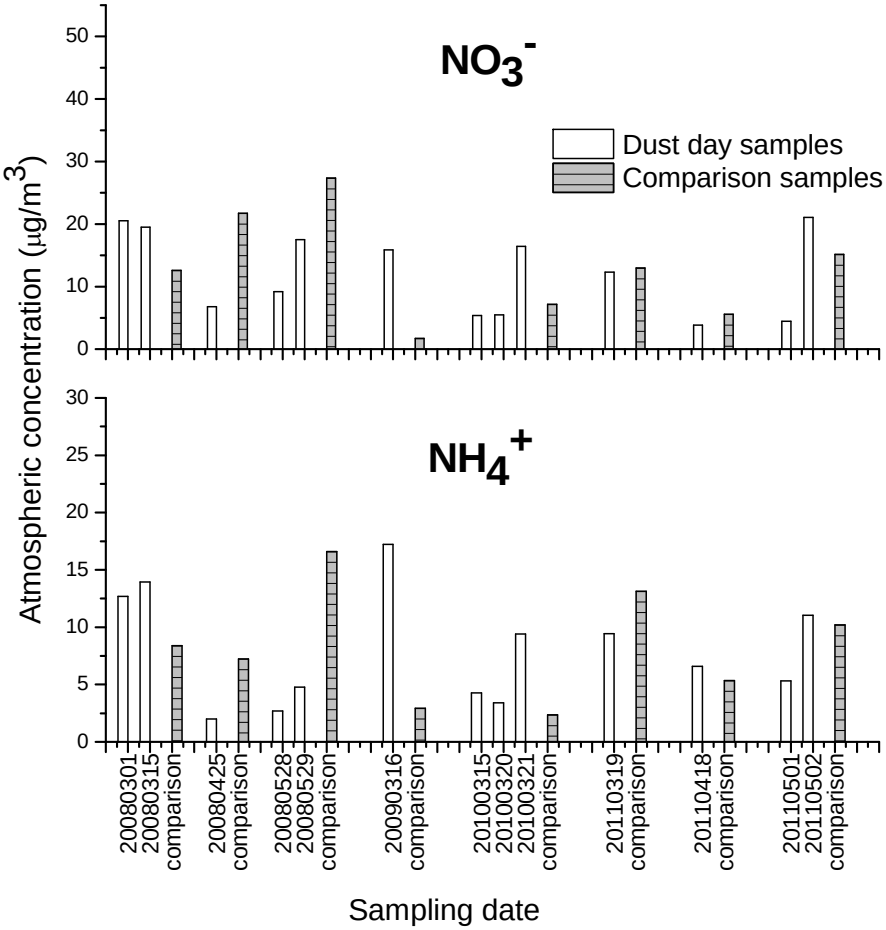

Figure 4. Mass concentrations of NH_4^+ andNO_3^-in aerosol samples collected at the Baguanshan site on dust and comparison days during March-May in 2008 to 2011.

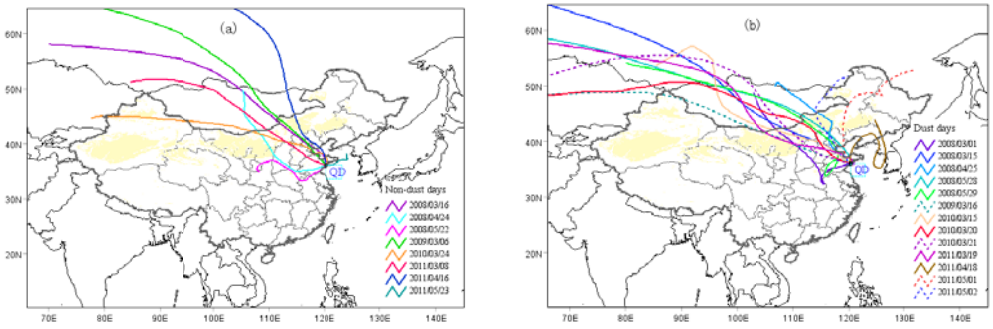

Figure 5. The 72-h backward trajectories for non-dust (a) and dust (b) samples from 2008 to 2011(the yellow domains in the maps represent the dust source regions in China).

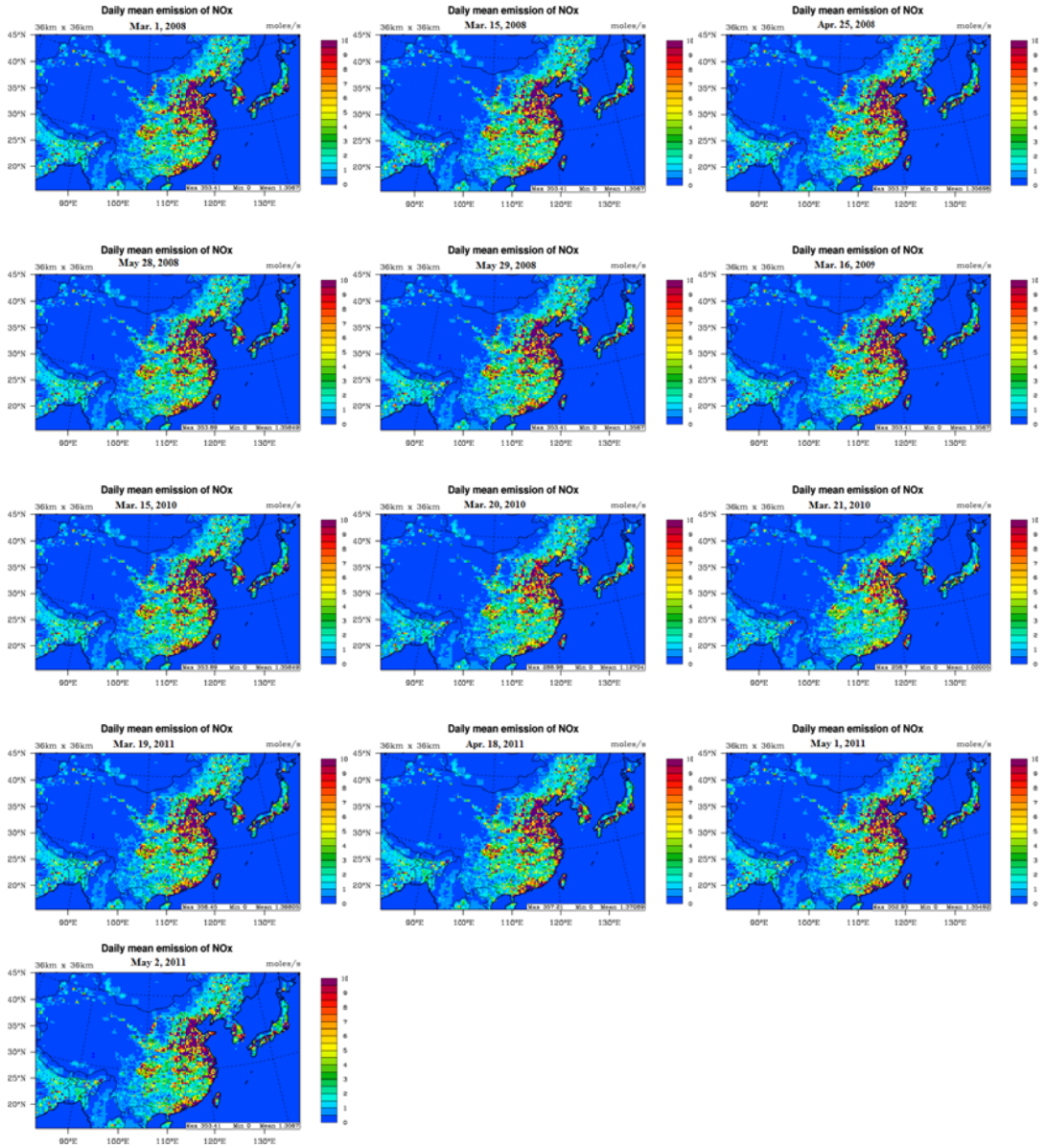

Figure 6. Daily mean emission of NOx over East Asia on the dust days from 2008 to 2011.

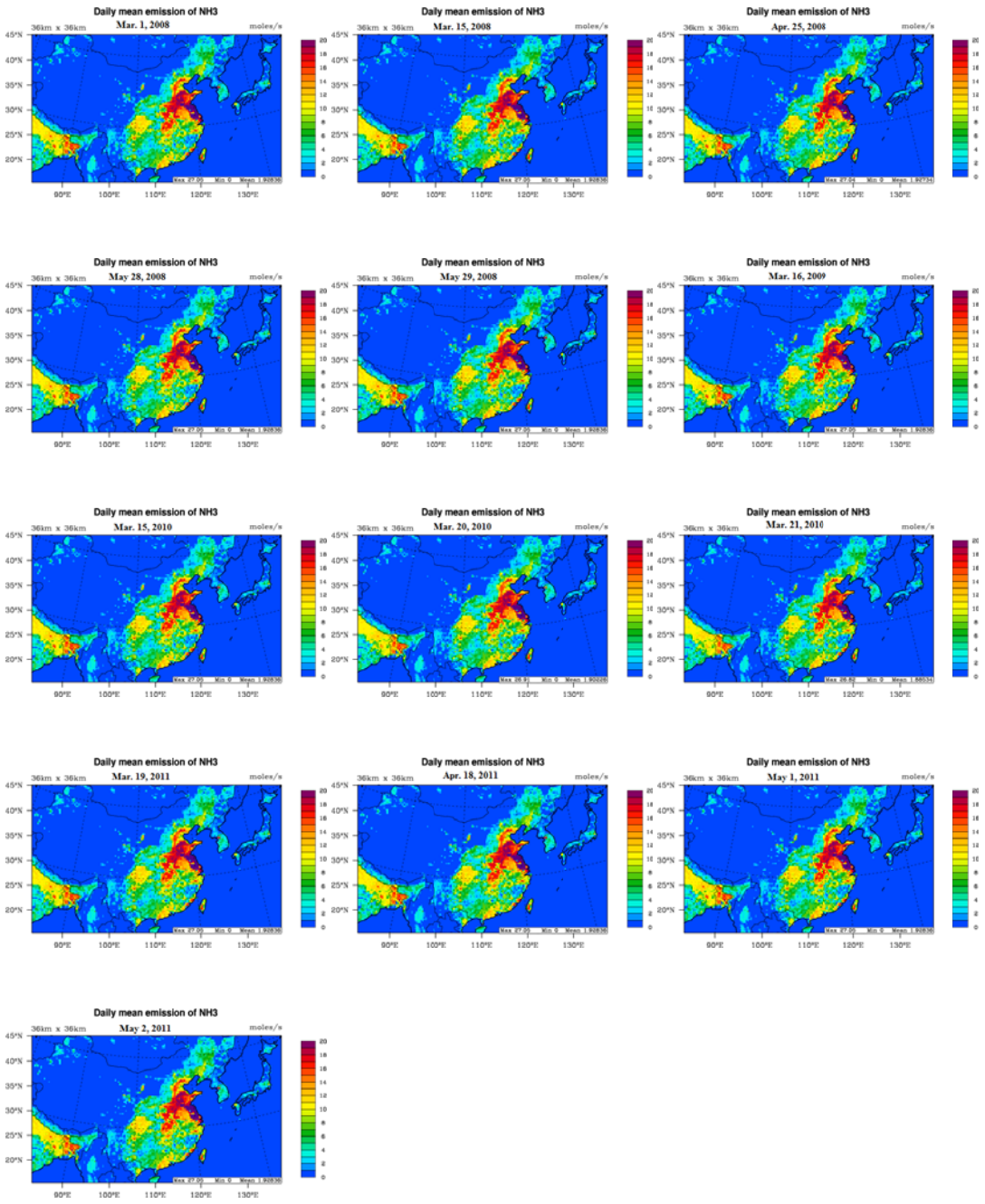

Figure 7. Daily mean emission of NH_3 over East Asia on the dust days from 2008 to 2011.

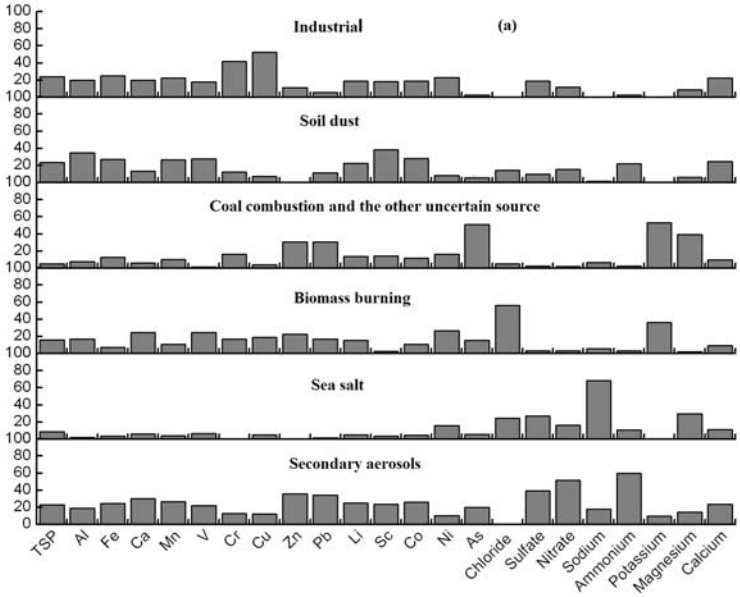

1017

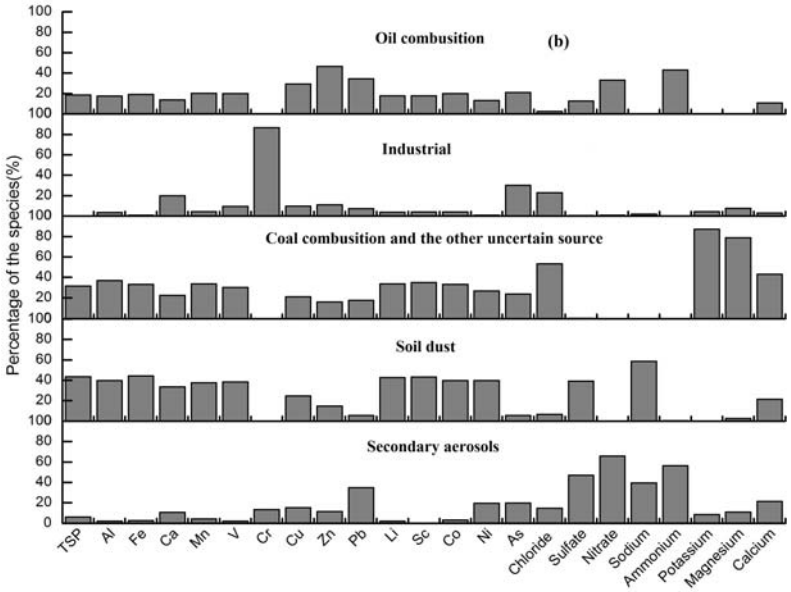

1018

1019

1020 **Figure 8.** Source profiles of atmospheric aerosol samples collected on non-dust (a) and dust (b) days
1021 using the PMF model

1022